Journal of Alloys and Compounds 506 (2010) 115–119

Contents lists available at ScienceDirect

Journal of Alloys and Compounds

journal homepage: www.elsevier.com/locate/jallcom

Microstructure development during directional solidification of Ti–45Al–8Nb alloy

X.F. Ding, J.P. Lin*, L.Q. Zhang, H.L. Wang, G.J. Hao, G.L. Chen

State Key Laboratory for Advanced Metals and Materials, University of Science and Technology Beijing, Beijing 100083, China

ARTICLE INFO

Article history:
Received 9 April 2010
Received in revised form 19 June 2010
Accepted 24 June 2010
Available online 3 July 2010

Keywords:
Intermetallics
Quenching
Phase transitions
Microstructure

ABSTRACT

Microstructure development and phase transition were investigated by quenching during directional solidification (DS) of Ti–45Al–8Nb (at.%) alloy. The solidification route and process can be controlled by adjustment of the solidification condition. A coexisted region of L + β + α was found at a low growth rate. The high temperature α phase, produced by peritectic transformation or β → α solid-state transformation or direct solidification from interdendritic liquid, was determined by the solidification conditions and can be identified by checking the β-segregation pattern in dendritic region. Lamellar orientation control was achieved when the interdendritic α grew on the top of peritectically formed α. High temperature α can be aligned continuously although α partly grew from the region of primary β interdendrite. Some elongated B2 particles were generated due to β-stablizers were centralized in interdendritic liquid during DS process. The volume fraction of the B2 particle decreased with decreasing growth rate (*V*).

1. Introduction

Niobium-rich TiAl-based alloys extensively attracted attentions in recent years for their excellent high temperature strength and oxidation resistance [1,2]. However, RT ductility and workability are poor which restricts their widespread applications on turbine engines and aerial materials [3]. A good combination of room temperature strength, ductility, toughness and creep strength can be achieved when the lamellar orientation is aligned parallel to the tensile direction [4–6]. Previous studies have shown that the lamellar orientation is closely related to the solidification route and process [7]. Directional solidification (DS) allows a close control of the microstructure and thus of the properties of the material since both the solidification route and process can be controlled by modifying the parameter during DS process.

In order to achieve the required lamellar orientation, the orientation of the high temperature α phase must first be controlled [8]. However, Nb addition induces the formation of new phase and changes the Ti–Al phase diagram, leading to a solidification route which is different to conventional TiAl alloys. During DS process with primary β alloy, high temperature α can be produced by the ways as follows: the peritectic reaction or transformation of L + β(Ti) → α(Ti), the solid-state transformation of β → α, the direct growing from the liquid and the combinations of above-mentioned. The orientation of the high temperature α phase is determined by the procedure in which it formed.

This paper gives a preliminary study on control of solidification process and thus of lamellar orientation with niobium-rich TiAl-based alloy using a DS technique. We report on experimental investigations of high temperature α grain's formation in primary β alloy and its effects on control of lamellar orientation during the DS process ended by quenching. The phase transformation and microstructure development in quenched mushy zones, especially the formation of elongated B2 particles during the DS process, were also discussed.

2. Experimental procedure

The intermetallic Ti–45Al–8Nb (at.%) alloy with the chemical composition of Ti–45.27Al–8.39Nb (at.%) was supplied in the form of plasma arc melting (PAM) cylindrical ingot. The oxygen content of the ingot was less than 640 ppm. The ingot was cut to smaller bars, and each one is typically 6.5 mm in diameter and 100 mm in length. The bars were placed into alumina crucibles which had been moulded by yttria. After heating-up and after a holding period of 15 min, DS experiments were carried out with a Bridgeman type apparatus under protection of 380 Pa high-purity argon. Fig. 1 shows the sketch of a Bridgeman type DS apparatus for TiAl alloys. The DS bars were grown under a measured temperature gradient in liquid $G_L = 5.2 \times 10^3$ K/m, and at the growth rates (*V*) of 10 and 100 μm/s respectively. The temperature gradient was determined by a W-Re5/26 thermocouple. After directional solidification to a constant length of 50 mm, they were quenched by a rapid displacement of the mould into the liquid metal bath.

The DS bars were sectioned longitudinally and transversely, polished using standard metallographic techniques. Microstructure analyses were conducted with the use of field emission scanning electron microscope (FEM) employing the back-scattered electron (BSE) imaging. Compositions of the various microstructural constituents were determined by electron probe micro-analyzer (EPMA).

* Corresponding author. Tel.: +86 10 62332192; fax: +86 10 62333447.
E-mail address: linjunpin@skl.ustb.edu.cn (J.P. Lin).

0925-8388/$ – see front matter © 2010 Elsevier B.V. All rights reserved.
doi:10.1016/j.jallcom.2010.06.151

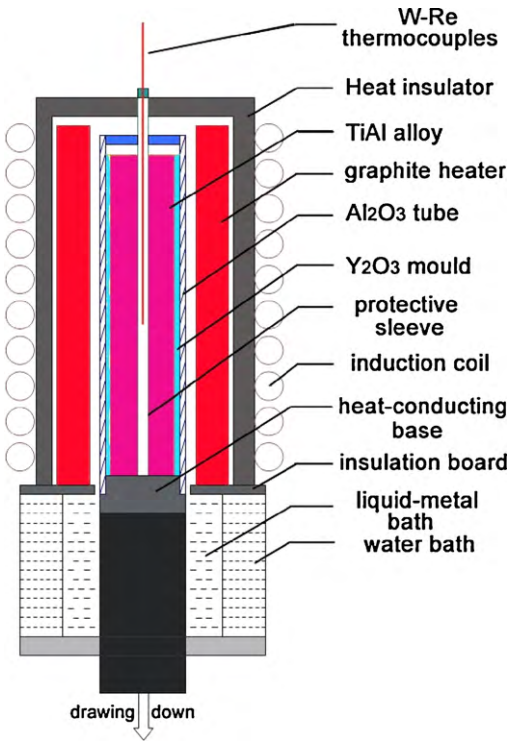

Fig. 1. Sketch of a Bridgeman type DS apparatus for TiAl alloys.

3. Results and discussion

3.1. Phase transition

Fig. 2 shows the typical microstructures in quenched mushy zones of the bars at the growth rate of 10 and 100 μm/s. Some Y_2O_3 particles were dropped into the melt due to the thermal impaction and convection applied to the yttria mould. Because quenching allows freezing-in the high temperature phases and preserving the mushy zone for subsequent analysis, the solidification route can be clearly distinguished by checking the microstructures on longitudinal section of the quenched bars at the growth rates of 10 and 100 μm/s.

As seen in Fig. 2, dendritic morphologies were found at both of the solid/liquid fronts. Cubic β was easily found to be the primary solidification phase in this alloy by noting that the secondary dendritic arms are orthogonal to the primary arms. During primary β solidification, Ti and Nb are segregated into the dendrites and Al is rejected into the interdendrites. According to the 8Nb–TiAl (at.%) quasi-phase diagram [9], an equilibrium solidification of Ti–45Al–8Nb alloy should lead to the following solidification sequence:

$$\text{Liq.} \rightarrow \text{Liq.} + \beta \rightarrow \beta \rightarrow \beta + \alpha \rightarrow \alpha \rightarrow \alpha + \gamma \rightarrow \text{lamella}(\alpha_2 + \gamma) + \gamma \quad (1)$$

However, it was found that liquid, α and β can coexist with each other in a region at lower growth rate of 10 μm/s (Fig. 2(a)). The peritectic transformation took place at the coexisted region of L + β + α. Peritectic phase α enveloped primary phase β by peritectic reaction at positions in the growth direction behind the β tips. Following by further decrease of temperature, γ was initially precipitated from the interdendritic Al-rich regions. At the higher growth rate of 100 μm/s, the peritectic transformation was only found at the border of the dendrite (Fig. 2(b)). Solid-state transformation of β → α can be identified in dendrites. Detail analysis will be presented later. Local enrichment of interdendritic liquid by Al induces to formation of γ phase. So two different routes of high temperature phase transition for studied alloy can be described in the forms:

$$\text{Liq.} \rightarrow \text{Liq.} + \beta \rightarrow \text{Liq.} + \beta + \alpha \rightarrow \alpha \rightarrow \alpha + \gamma \quad (2)$$

$$\text{Liq.} \rightarrow \text{Liq.} + \beta \rightarrow \alpha(\text{dendritic}) + \gamma(\text{interdendritic}) \quad (3)$$

The cellular coupled growth is found at higher G/V ratios, however, the dendritic microstructure with a peritectic phase enveloped primary dendrites with signs of partial solid-state transformation is usually found at lower G_L/V ratios [10]. As shown by the arrow 1 in Fig. 2(a), the liquid in the interdendritic region is easier and first to peritectically react with the β at the β–liquid interface. Peritectic transformation occurs when primary β is isolated by peritectic α. It is suggested that the driving force of diffusion resulting from the high temperature may be so large that the peritectic transformation is very fast in the beginning. But it slows down rapidly and is hardly completed due to the low diffusion coefficient in the solid phase (as shown by the arrow 2). A small volume fraction of residual β phase was eventually formed in the dendritic cores. Peritectic

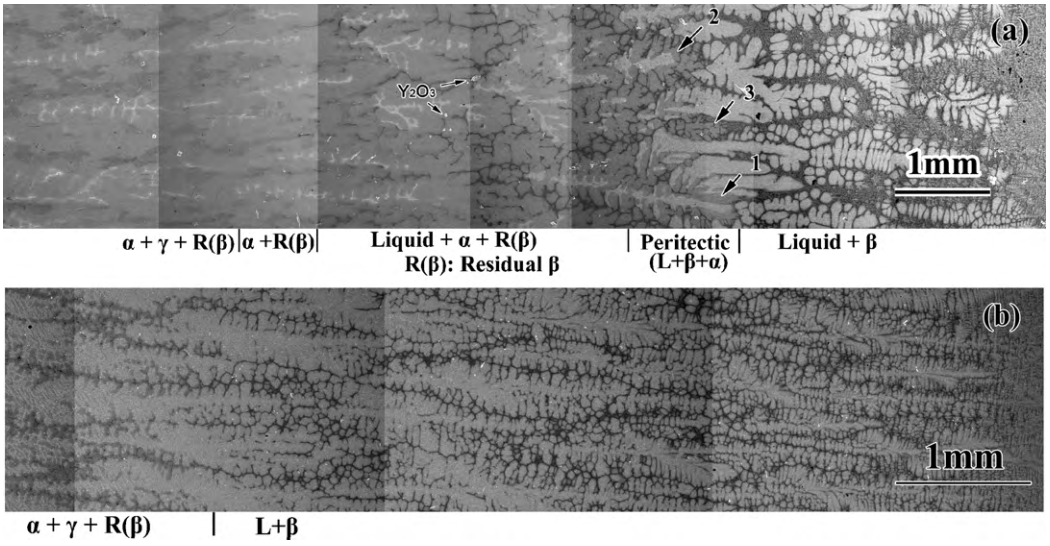

Fig. 2. BSE microstructures in quenched mushy zones in longitudinal sections of the bars at the growth rate of (a) 10 μm/s and (b) 100 μm/s.

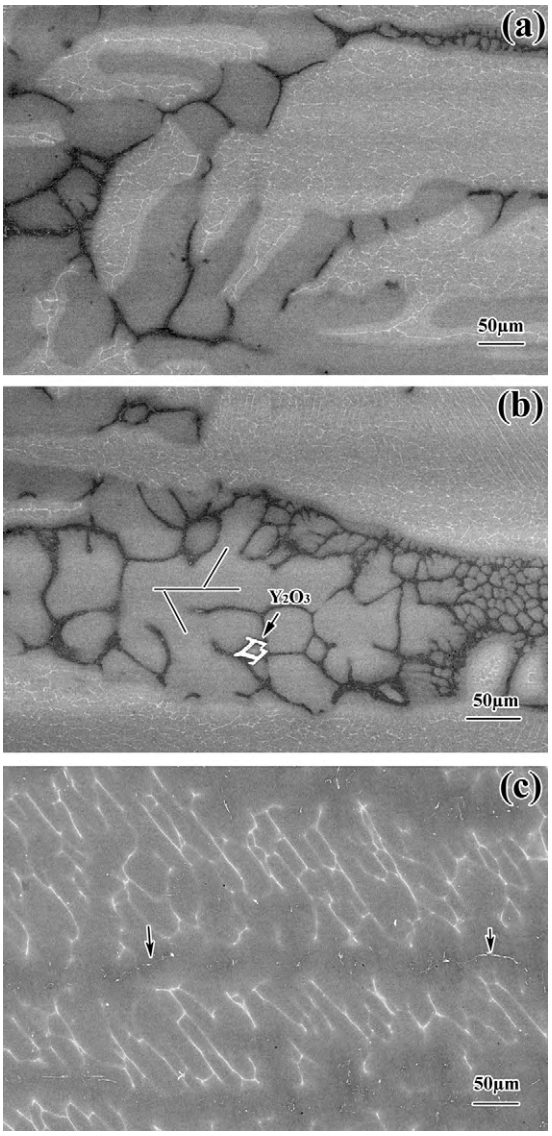

Fig. 3. The morphologies of quenched α in different procedures: (a) peritectic transformation, (b) direct solidification from interdendritic liquid and (c) β → α solid-state transformation.

phase α can also be produced by direct solidification from the liquid as well as peritectic reaction and transformation. The fraction of peritectic phase formed by direct solidification increases with increasing growth rate.

Fig. 3 shows the morphologies of quenched α in different procedures. The microstructure, which had finished the peritectic transformation, can be easily recognized because there is no residual β phase in it. As indicated by Chen et al. [11], β → α transformation can result in several α grains were nucleated in a single β grain and β-segregation were formed at the interface between the β and the α grains. The residual β in peritectic transformation will also result in subsequent β → α solid-state transformation during quenching. The region of quenched residual β in Fig. 3(a) has shown the pattern of β-segregation, which is similar to pattern of β-segregation in Figs. 2(b) and 3(c). So the pattern of β-segregation can enlighten us to recognize which transformation procedure has been experienced during DS process. It is related to the peritectic transformation when the pattern centralized in dendritic cores, and it is induced by β → α transformation when the pattern displayed a reticular morphology spread over the dendritic regions. The quenched α growing from interdendritic liquid can be easily identified by noting that no β-segregation existed in its dendritic region. Sometimes, even its secondary arms inclined at an angle of 60° to the primary dendrite spines can also be found (Fig. 3(b)) and that should be caused by growing hcp α phase from the liquid. The compositions of quenched α produced by peritectic transformation, direct growing from interdendritic liquid and β → α transformation were summarized in Table 1.

Table 1
The compositions of quenched α produced by different procedures.

Quenched α grain	Elemental composition (at.%)		
	Ti	Al	Nb
Peritectically transformed	44.52 ± 0.27	47.06 ± 0.26	8.42 ± 0.66
Growing from interdendritic liquid	44.29 ± 0.26	47.37 ± 0.26	8.34 ± 0.66
β → α transformed	44.16 ± 0.25	45.99 ± 0.27	9.85 ± 0.67

3.2. Control of lamellar orientation

Takeyama et al. have attempted to control the lamellar orientation in TiAl alloys by the DS with or without a seeding technique [7,12]. They have experimentally revealed that the lamellar orientation of a single crystal (PST) can be achieved by controlling the orientation of α crystal [13,14]. As to the TiAl alloy with primary β solidification, Jung et al. have proposed that the fully transformation to β from the liquid is the requirement in modifying the solidification process [15]. However, it is difficulty to control the fully β transformation for two reasons: one is that α crystal could grow from the β interdendritic liquid [16], the other is that the peritectic reaction and transformation restrain the primary β growing

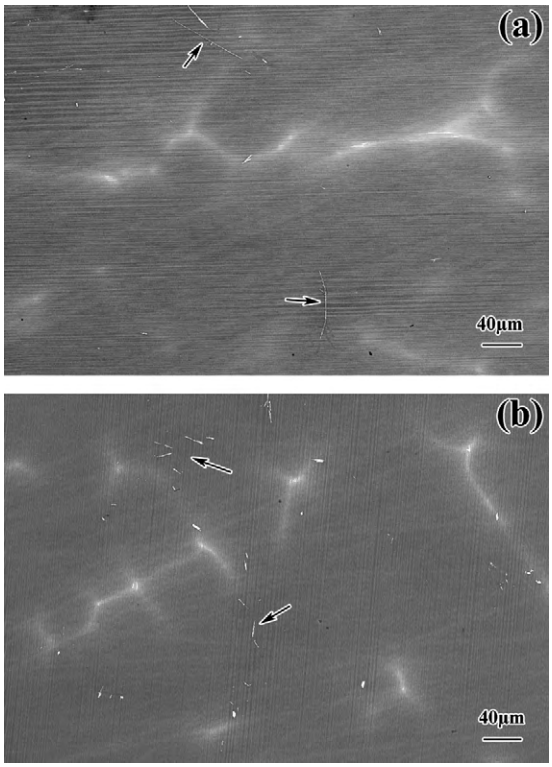

Fig. 4. Room temperature microstructures of the DS bar at the growth rate of 10 μm/s: (a) on the longitudinal section and (b) on the transversal section.

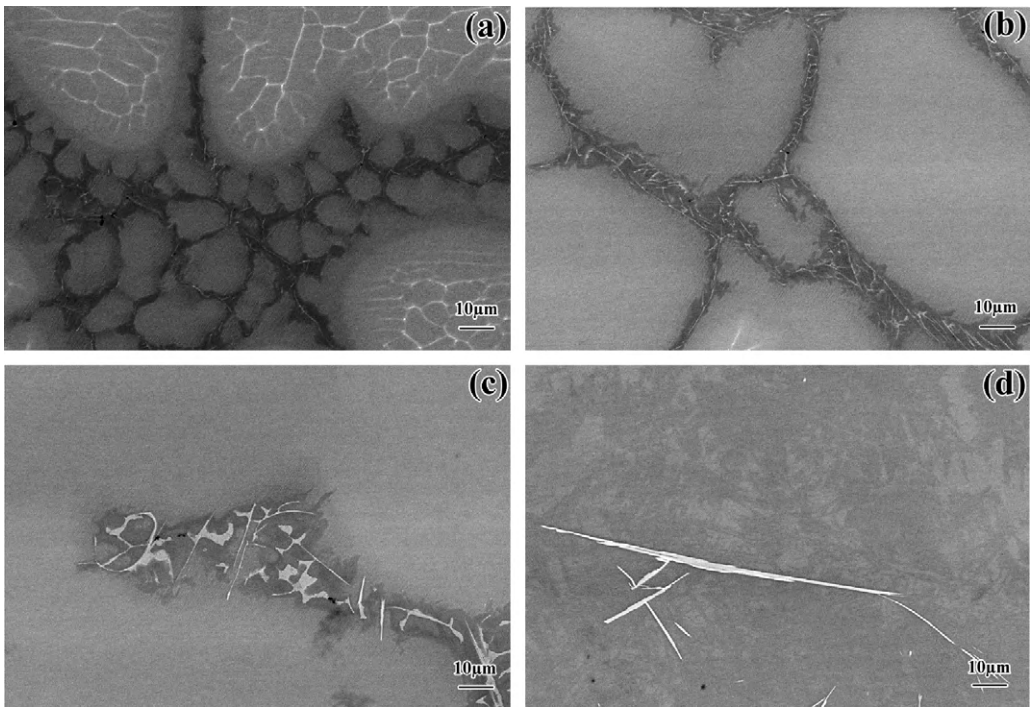

Fig. 5. The quenched interdendritic microstructures in different regions: (a) L + β, (b) L + β + α, (c) L + α + R(β) and (d) α + γ + R(β).

up, what induces to the discontinuous α formed in the β dendritic and interdendritic regions. Both of them will result in formations of the variant α crystals with different orientations.

It is obviously against to align the orientation of α by $\beta \rightarrow \alpha$ transformation because its variants with different orientations will be generated. But in the DS bar with $L + \beta \rightarrow \alpha$ peritectic transformation, the lamellar orientation was found to be well aligned. Fig. 4 shows the room temperature microstructures on the longitudinal and transversal sections of the bar at the growth rate of 10 μm/s. The lamellar boundary is not changed in the regions of β-segregation and original primary β interdendrite. A well aligned lamellar orientation was found in the DS bar without $\beta \rightarrow \alpha$ solid-state transformation. The procedure of partly transformation to β with α crystal growing from the interdendritic region is clearly shown in Fig. 2(a). As shown by the arrow 3, no residual β in α dendritic core which indicates that the α dendrite should not be produced by the peritectic transformation, but should grow from the liquid. The dendritic tip has changed acute and gradually occupied the original β interdendritic regions. As shown by the arrow 2 in Fig. 2(a), the peritectially formed α is well connected with the α growing from liquid so as to form a continuous dendritic arm. Therefore, it is reasonably concluded that the interdendritic α should grow on the top of peritectically formed α and eventually align the high temperature α phase, which is responsible for the successful controlling of lamellar orientation in this type of β solidification alloy. High Nb addition has increased the temperature of pectectic reaction so that the peritectically formed α can possibly be formed before the formation of the interdendritic α phase.

3.3. Formation of elongated B2 (ordered β) particle

As shown in Figs. 3(c) and 4, some elongated B2 particles was usually found in the interdendritic regions at a lower or higher growth rate. They were also found by Lapin et al. in microstructures of the TiAl alloys containing β-stabilizer elements [17,18]. These particles could greatly affect the mechanical properties of the lamellar structure. They not only changed the local temperature at which the lamellar structure form, and thus a coarser lamellar structure would obtained around the B2 particles (Fig. 4), but also were likely to cause stress concentration, and larger B2 particles will be possibly detrimental to the ductility. So it is necessary to find out the process in which these particles are formed.

Fig. 5 shows the quenched interdendritic microstructures in different regions of the growth stages. As shown in Fig. 5(a), Al enrichment in interdendritic liquid leads to formation of γ phase during quenching. Several γ grains were found in the interdendritic area and a small volume fraction of white contrast phase was also found around the γ after quenching. Hence, not all of the β-stablizers were concentrated into the β dendrites when β grew from the liquid. The interdendritic liquid was consumed by peritectic reaction and growing of α. A strip phase initially participated in liquid when the interdendritic β-stablizers were in a supersaturated solution in the region of L + β + α (Fig. 5(b)). They were inclined to be combined into coarse ones for the surface tension of the liquid (Fig. 5(c)). The diffusion of Al from liquid to α accelerated the tendency of β-stablizers centralization until the interdendritic liquid was consumed over. Further decreased temperature greatly decreased β-stablizers diffusion in solid-state phase and then elongated β particles were eventually formed in interdendrites in α + γ + R(β) region (Fig. 5(d)).

Increase of growth rate can bring about departure from equilibrium solidification and increase the solute segregation. Solute rejection of the tips increases with growth rate leading to increasing undercooling [19]. β-Stablizers in interdendritic region are easier to reach in a supersaturated solution and more difficulty to diffuse at a low temperature. So the volume fraction of B2 particles will decrease with decreasing growth rate.

4. Conclusions

1. The solidification route and process can be controlled during directional solidification of primary β Ti–45Al–8Nb (at.%) alloy. A coexisted region of L + β + α was found at a lower growth rate. The high temperature α phase, which was generated by peritec-

tic transformation or $\beta \rightarrow \alpha$ solid-state transformation or direct solidification from interdendritic liquid, was determined by the solidification conditions and can be identified by checking the β-segregation pattern in dendritic region.

2. Lamellar orientation can be controlled when the interdendritic α grew on the top of peritectically formed α. High temperature α was aligned continuously although partly β transformed from the liquid.
3. Some elongated B2 particles were formed by β-stablizers centralization in interdendritic liquid during DS process. The volume fraction of the B2 particles decreases with decreasing growth rate.

Acknowledgements

This work was supported by the National Natural Science Foundation of China under contracts No. 50771013 and No. 50871127.

References

[1] J.P. Lin, X.J. Xu, Y.L. Wang, S.F. He, Y. Zhang, X.P. Song, G.L. Chen, Intermetallics 15 (2007) 668–674.
[2] M. Yoshihara, K. Miura, Intermetallics 3 (1995) 357–363.
[3] X.J. Xu, J.P. Lin, Y.L. Wang, J.F. Gao, Z. Lin, G.L. Chen, J. Alloys Compd. 414 (2006) 131–136.
[4] D.R. Johnson, H.N. Lee, S. Muto, T. Yamanaka, H. Inui, M. Yamaguchi, Intermetallics 9 (2001) 923–927.
[5] H.N. Lee, D.R. Johnson, H. Inui, M.H. Oh, D.M. Wee, M. Yamaguchi, Intermetallics 10 (2002) 841–850.
[6] K. Kishida, D.R. Johnson, Y. Masuda, H. Umeda, H. Inui, M. Yamaguchi, Intermetallics 6 (1998) 679–683.
[7] M.C. Kim, M.H. Oh, J.H. Lee, H. Inui, M. Yamaguchi, D.M. Wee, Mater. Sci. Eng. A 239–240 (1997) 570–576.
[8] D.R. Johnson, H. Inui, S. Muto, Y. Omiya, T. Yamanaka, Acta Mater. 54 (2006) 1077–1085.
[9] G.L. Chen, W.J. Zhang, Z.C. Liu, S.J. Li, Y.W. Kim, in: Y.W. Kim, D.M. Dimiduk, M.H. Loretto (Eds.), Gamma Titanium Aluminides, TMS, Warrendale, PA, 1999, pp. 371–380.
[10] S. Dobler, T.S. Lo, M. Plapp, A. Karma, W. Kurz, Acta Mater. 52 (2004) 2795–2808.
[11] G.L. Chen, X.J. Xu, Z.K. Teng, Y.L. Wang, J.P. Lin, Intermetallics 15 (2007) 625–631.
[12] M. Yamaguchi, D.R. Johnson, H.N. Lee, H. Inui, Intermetallics 8 (2000) 511–517.
[13] Y. Yamamoto, M. Takeyama, Intermetallics 13 (2005) 965–970.
[14] A. Takeyama, Y. Yamamoto, H. Morishima, K. Koike, S.Y. Chang, T. Matsuo, Mater. Sci. Eng. A 329–331 (2002) 7–12.
[15] I.S. Jung, H.S. Jang, M.H. Oh, J.H. Lee, D.M. Wee, Mater. Sci. Eng. A 329–331 (2002) 13–18.
[16] D.R. Johnson, K. Chihara, H. Inui, M. Yamaguchi, Acta Mater 46 (1998) 6529–6540.
[17] J. Lapin, L. Ondr, M. Nazmy, Intermetallics 10 (2002) 1019–1031.
[18] H.N. Lee, D.R. Johnson, H. Inui, M.H. Oh, D.M. Wee, M. Yamaguchi, Mater. Sci. Eng. A 329–331 (2002) 19–24.
[19] T. Umedaa, T. Okanea, W. Kurz, Acta Mater. 44 (1996) 4209–4216.